RSC Advances

This is an *Accepted Manuscript*, which has been through the Royal Society of Chemistry peer review process and has been accepted for publication.

Accepted Manuscripts are published online shortly after acceptance, before technical editing, formatting and proof reading. Using this free service, authors can make their results available to the community, in citable form, before we publish the edited article. This *Accepted Manuscript* will be replaced by the edited, formatted and paginated article as soon as this is available.

You can find more information about *Accepted Manuscripts* in the Information for Authors.

Please note that technical editing may introduce minor changes to the text and/or graphics, which may alter content. The journal's standard Terms & Conditions and the Ethical guidelines still apply. In no event shall the Royal Society of Chemistry be held responsible for any errors or omissions in this *Accepted Manuscript* or any consequences arising from the use of any information it contains.

ROYAL SOCIETY OF CHEMISTRY

www.rsc.org/advances

Effects of Silica-coated Carbon Nanotubes on the Curing Behavior and Properties of Epoxy Composites

[1] Ao Li, Weizhen Li*, Yang Ling, Wenjun Gan*

College of Chemistry and Chemical Engineering, Shanghai University of Engineering Science, 333 Longteng Road, Shanghai, 201620, China

[2] Michael A. Brady, Cheng Wang

Advanced Light Source, Lawrence Berkeley National Laboratory, 1 Cyclotron Road, Berkeley, CA 94720, USA

RSC Advances Accepted Manuscript

Corresponding author. Tel.: +86 21 67791217; fax: +86 21 67791214.

E-mail address: liweizhen@sues.edu.cn, wjgan@sues.edu.cn

Abstract: Multi-walled carbon nanotubes (MWCNTs) were coated with silica by a sol-gel method to improve interfacial bonding and dispersion of nanotubes in diglycidyl ether of bisphenol A (DGEBA) matrix. TEM and FE-SEM measurements showed that the silica shell was successfully coated on the surface of r-MWCNTs (as-received MWCNTs), and that the dispersion of MWCNT@SiO_2 in the epoxy matrix and interfacial adhesion between MWCNTs and epoxy were improved through the silica shell formation. The effects of silica-coated multi-walled carbon nanotube (MWCNT@SiO_2) addition on the curing behavior of epoxy resin, and on the physical and thermomechanical properties of epoxy composites, were studied. FT-IR measurements of different blends at different curing times indicated that the curing reaction was accelerated with the presence of MWCNTs and increased with the content of MWCNT@SiO_2. DSC results confirmed that the value of activation energy decreased with the introduction of MWCNTs in the order of MWCNT@SiO_2 < r-MWCNTs < epoxy. It was found that the thermal conductivity of epoxy composites were significantly enhanced by incorporation of MWCNT@SiO_2, relative to composites with r-MWCNTs, while the values of glass transition temperature slightly increased, and the high electrical resistivity of these composites was retained overall.

Keywords: Silica-coated multi-walled carbon nanotube, Epoxy composite, Curing behavior, Physical and thermomechanical properties

RSC Advances Accepted Manuscript

1. Introduction

Carbon nanotubes (CNTs), discovered in 1991 by Iijima [1], are often referred to as one-dimensional materials because of their high aspect ratio and have excellent mechanical properties, such as high elastic modulus and high tensile strength. They are considered to be the most promising reinforcement fillers for polymer matrices in improving their mechanical properties [2-5]. Meanwhile, CNTs have unusually high electrical and thermal conductivity [2-4,6-7] due to out-of-plane delocalized π electrons, σ - π rehybridization [2], and phonon-dominated ballistic heat transport [5,7-9].

As an important class of thermosetting polymers for high performance composites and electrical applications, epoxy resins show excellent electrical insulation properties, good chemical resistance, high adhesion, and low curing shrinkage. Incorporation of CNTs into epoxy resin has proven to be a good strategy for obtaining polymer composites with favorable mechanical properties [10-13], good thermal conductivity [14-18], and improved toughness [19-22].

Among the various polymer composites, epoxy-based systems are very important materials for electronic packaging applications. For such applications, thermally conducting but electrically insulating materials are required. The common advantage of CNTs being electrically conductive is no longer desired. A facile method for improving thermal conductivity while retaining high electrical resistivity is to incorporate silica-coated carbon nanotubes (CNT@SiO_2) into the epoxy system [9,23-24]. Silica has been widely used as a filler in electronic packaging material. Silanized or silica-coated nanotubes can not only improve the interfacial adhesion between the CNTs and matrix and the resulting dispersion of CNTs in epoxy, but also improve the composite's electrical, thermal, and mechanical properties [24-26]. Although previous

RSC Advances Accepted Manuscript

studies showed a functional layer on the CNT surface, providing a predicted reinforcement and improvement of thermal conductivity and electrical resistivity, the influence of the silica coating at the CNT surface on the curing behavior is still not well understood.

The incorporation of CNTs as reinforcement will surely enhance the mechanical and thermal properties of epoxy resins but would also modify their processing behavior. Characterization of the curing kinetics of the CNT-filled epoxy resin is one of the prerequisites for designing and optimizing the process parameters. Studies have been reported on the curing behavior of CNT/epoxy [27-31] and surface treated-CNT/epoxy systems [32-37]. However, fewer reports exist regarding the effect of silica-coated CNTs on the curing behavior of epoxy composite resin.

Moreover, anhydride-cured epoxy resins show improved properties over amine-cured resins, such as electrical insulation, low exotherms and shrinkage during curing, as well as low water absorption and nearly internal stress-free materials after curing. Therefore, anhydride-cured systems are widely used as electrical insulation materials [38]. Although anhydride hardeners have been employed for CNT/epoxy composites [39-40], further study on the anhydride curing behavior is needed.

In this study, a simple sol-gel method was used to obtain silica-coated MWCNTs (MWCNT@SiO_2) directly from r-MWCNTs (as-received carboxylated MWCNTs), which was characterized by transmission electron microscopy (TEM). Anhydride-cured epoxy composites modified with r-MWCNTs (r-MWCNT/epoxy composites are used as an additional 'control' formulation, as no silica coating is present in these composites) and MWCNT@SiO_2 are then prepared and imaged by scanning electron microscopy (SEM) and TEM. Subsequently, the curing process is monitored with Fourier transform infrared spectroscopy (FT-IR) and differential scanning calorimetry

RSC Advances Accepted Manuscript

(DSC). The effects of various contents of r-MWCNTs and MWCNT@SiO_2 on the curing behavior will be discussed. Finally, the effects of various contents of r-MWCNTs and MWCNT@SiO_2 on the thermomechanical properties, electrical resistivity, and thermal conductivity are evaluated.

2. Experimental

2.1 Materials

Carboxylated MWCNTs, supplied from Shenzhen Nanotech Port Co. Ltd., with carboxylic groups on the surface and a diameter of 20-40 nm and length of 2-5 μm, were used as-received (r-MWCNTs) directly because of their enhanced dispersibility. Tetraethylorthosilicate (TEOS), ethanol, ammonia, and other chemical reagents were of analytical grade and supplied from Shanghai Reagents Co., China.

A commercial epoxy resin (DER 331, with an epoxide equivalent weight of 182-192 g/mol) from Dow Chemical and a curing agent methyltetrahydrophthalic anhydride (MTHPA) and accelerator benzyldimethylamine (BDMA), from Shanghai TCI Chemical Industry Co. Ltd., were used without further purification.

2.2 Synthesis of silica-coated MWCNTs (MWCNT@SiO_2)

MWCNT@SiO_2 was prepared by the sol-gel method by reference to the reported literatures [41-42]. 100 mg of r-MWCNTs was firstly ultrasonically dispersed into 30 mL of deionized water for 1 h. The suspension was then added to 80 mL of ethanol and ultrasonicated for another 0.5 h to form a stable dispersion. Immediately, 2 mL of $NH_3 \cdot H_2O$ was added into the as-prepared MWCNT dispersion. Next, a TEOS solution (1 mL of TEOS in 40 mL of ethanol) was dropped into the MWCNT dispersion under mechanical stirring, and the mixture was stirred for another 12 h at room temperature to complete the reaction. Finally, the mixture was centrifuged and washed with

RSC Advances Accepted Manuscript

ethanol repeatedly to remove the free silica particles. These processes were expected to result in the formation of about 216 mg uniform and thick layer of silica on every individual MWCNT. The synthetic preparation of MWCNT@SiO_2 is presented in Fig. 1.

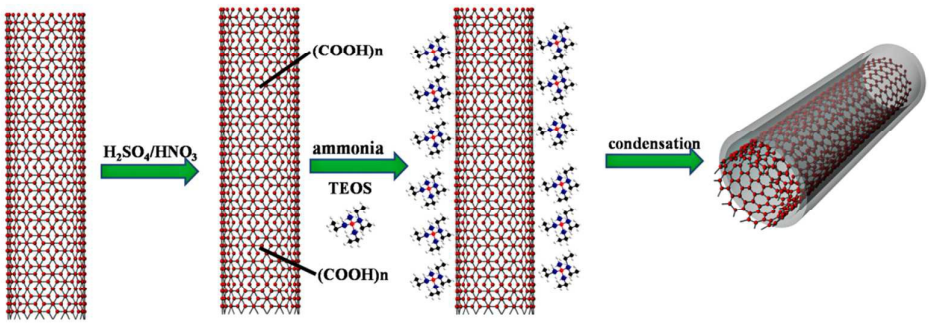

Fig. 1 The synthetic preparation of MWCNT@SiO_2.

2.3 Preparation of MWCNT/epoxy composites

MWCNT@SiO_2 (0.75, 1.5 and 2 wt% of epoxy composite) was dispersed in tetrahydrofuran (THF) for 30 min by means of ultrasonication at room temperature. The obtained dispersion was then added to the preheated epoxy resin (60 ºC) under ultrasonic vibration. Afterwards, the temperature was increased to 80 ºC, and the mixture was ultrasonicated for another 1 h, followed by intensive mechanical stirring for 1 h to ensure homogeneity and allow the THF to evaporate. The curing agent Me-THPA was then added at an epoxy-to-hardener ratio of 1:0.8 by weight, and the mixture was degassed under vacuum to remove any trapped air bubbles. Finally, the mixture was cast in aluminum moulds and cured at 80 ºC for 30 min, followed by curing at 150 ºC for another 5 h. Control samples of neat epoxy resin and r-MWCNT/epoxy composites were also prepared by the same procedure and

RSC Advances Accepted Manuscript

conditions.

2.4 Characterization and Measurement

TEM images were taken on a JEOL-2100F microscope to characterize the r-MWCNTs and MWCNT@SiO_2. The morphological observations of the sample fracture surface were carried out using a field-emission SEM (FESEM) (Hitachi Su-8010). The cryogenically fractured surfaces of the specimens were coated with platinum prior to their microscopy characterization.

The FT-IR spectra of r-MWCNTs, MWCNT@SiO_2, and composites modified with MWCNTs were recorded on a Nicolet AVATAR (Thermo Fisher, USA) with a wavenumber resolution of 4 cm^{-1}. The curing behavior of the epoxy resin with and without MWCNTs was studied by isothermal FT-IR at 150 ºC and nonisothermal DSC, using a PT-10 (Linseis, Germany) differential thermal analyzer, at various heating rates of 2.5, 5, 10, 15 and 20 K/min, in the range of 30-300 ºC, under nitrogen atmosphere.

Bulk electrical resistivity measurements were conducted using a plate electrode, type ZC36, high resistance meter (Shanghai Cany Precision Instrument Co., China). Thermal conductivity of the composites was measured at room temperature using a transient QTM-D2 heat-flow meter (SDK Co., Japan). Thermomechanical properties of the composites were evaluated by dynamic mechanical analysis (DMA) (TA Q800, USA) with a three-point bending mode. The heating rate was 3 ºC/min in a temperature range of 30-250 ºC, at a frequency of 1 Hz.

3. Results and Discussion

3.1 Characterization of MWCNTs and MWCNT@SiO_2

3.1.1 FT-IR analysis

RSC Advances Accepted Manuscript

FT-IR spectra for r-MWCNTs and MWCNT@SiO_2 are shown in Fig. 2. Carboxylic acid functional groups (-COOH) can be identified on the surface of the r-MWCNTs and MWCNT@SiO_2 by FT-IR spectroscopy. Vibrational modes at 3425/3417 and 1728/1718 cm^{-1} can be attributed to O-H stretching and carbonyl stretching of the carboxylic acid groups [13, 25], respectively. The spectra show that a certain amount of carboxylic acid groups are attached to both r-MWCNTs and MWCNT@SiO_2. Compared with r-MWCNTs, new obvious peaks at 2922 and 2852 cm^{-1} are observed, which can be attributed to C-H stretching and bending modes from the TEOS molecules, for MWCNT@SiO_2. Furthermore, the absorbance peaks at 1065, 964 and 793 cm^{-1} are also observed, which correspond to the Si-O-Si stretching and bending modes and the stretching of Si-OH groups, respectively, for the hydroxylated silica-coated nanotubes [25-26]. These new peaks suggest that the r-MWCNTs were indeed modified by the silica deposition.

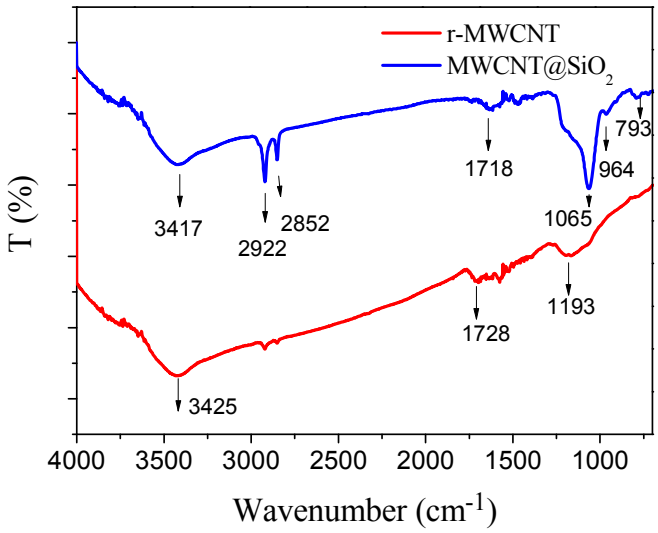

Fig. 2 FT-IR spectra of r-MWCNTs and MWCNT@SiO_2.

RSC Advances Accepted Manuscript

3.1.2 Morphology

The morphology of synthesized MWCNT@SiO_2 was observed and compared with r-MWCNTs using TEM, and the images are shown in Fig. 3. No obvious silica particles can be observed, and the entanglement between the tubes appears to be weak. The core/shell structure of MWCNT@SiO_2, with insulating silica as the shell and MWCNT as the core, can be observed in Fig. 3b and 3c. Fig. 3c is in low magnification of Fig. 3b to show the uniform coating of silica on MWCNT. The diameters of the tubes are with an average value of approximately 90 nm, while the length of the tubes is on the order of several micrometers. Thus, TEM indicates that a silica shell of approximately 30 nm thickness (20-40 nm diameter for r-MWCNTs, Fig. 3a) was successfully coated on the r-MWCNTs by the sol-gel process, and that the silica detected by FT-IR indeed exists as a coating on the outside surface of r-MWCNTs.

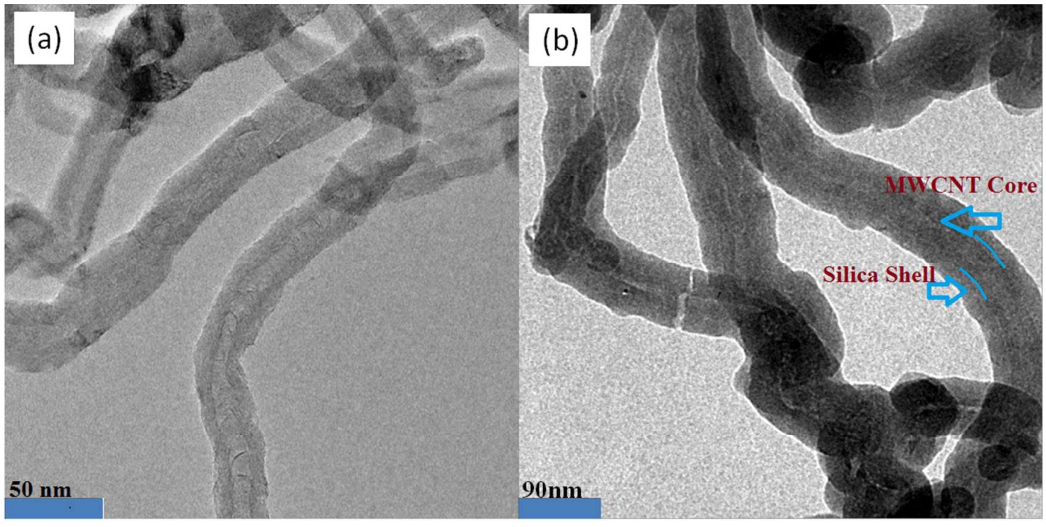

RSC Advances Accepted Manuscript

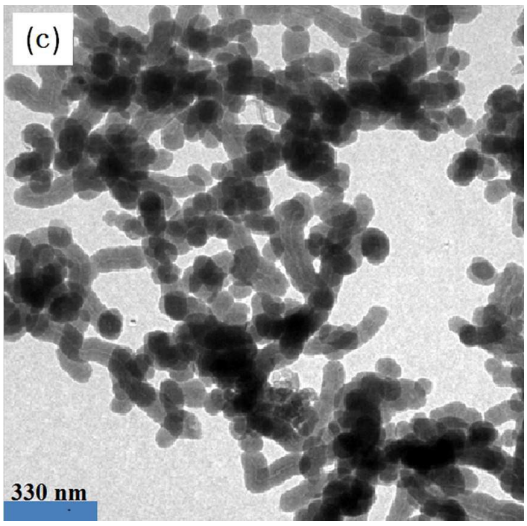

Fig. 3 TEM images of (a) r-MWCNTs, (b,c) MWCNT@SiO_2 in different magnification.

3.2 Composite characterization

3.2.1 Morphology of fracture surface

In order to investigate the dispersibility and the interfacial adhesion of MWCNTs in the epoxy matrix, the prepared epoxy composites were cryogenically fractured, and the morphology of the cross section was examined. Fig. 4 presents the representative SEM images of the fractured surfaces for the composites. It's obvious that the dispersibility is not the problem for composites with 0.75 wt% of CNTs (Fig. 4a, b).

RSC Advances Accepted Manuscript

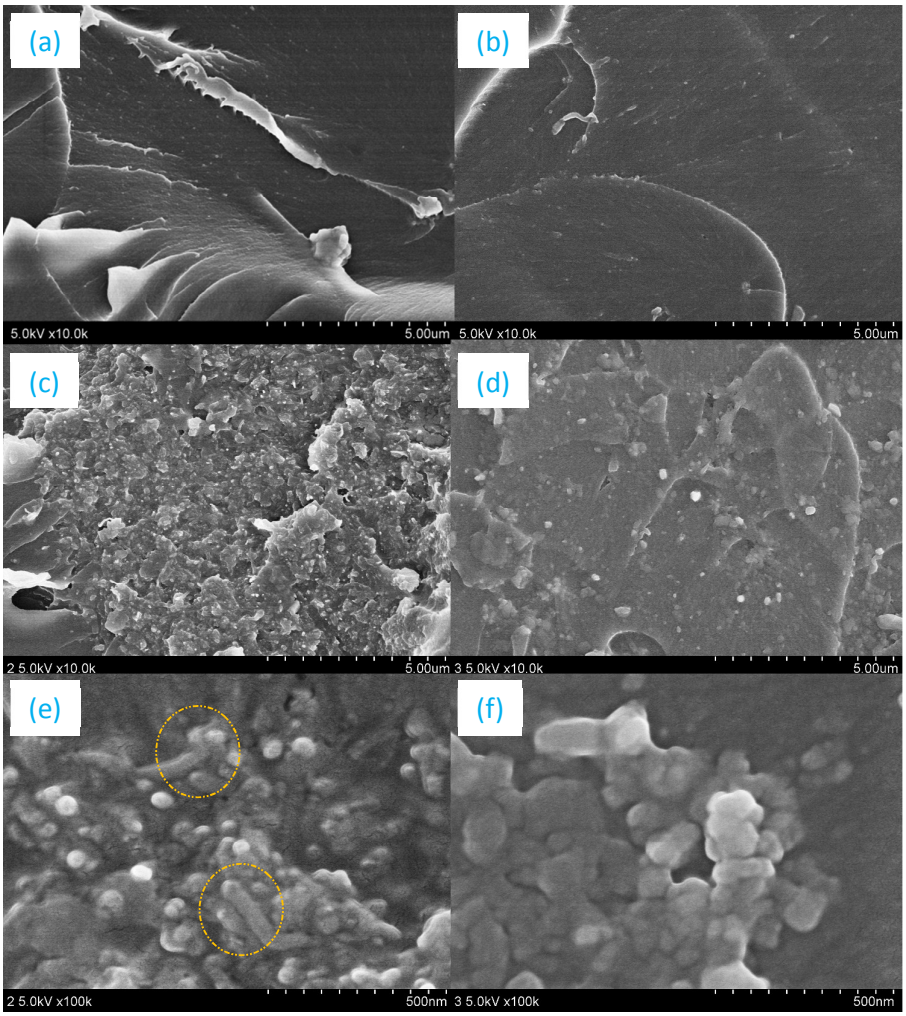

Fig. 4 FE-SEM images of the fracture surfaces for epoxy composites containing 0.75 wt% of (a) r-MWCNTs and (b) MWCNT@SiO_2, 2.0 wt% of (c,e) r-MWCNTs and (d,f) MWCNT@SiO_2. The yellow circles in (e) highlight nanotubes that have been pulled out from the matrix during the fracture process.

Still good dispersion of CNTs in the epoxy matrix with 2.0 wt% of r-MWCNTs can be seen in Fig. 4c, d. Fig. 4e indicates that r-MWCNTs are generally embedded in the epoxy matrix, and the interfacial adhesion between MWCNTs and epoxy are improved through the carboxylic acid surface chemistry of r-MWCNTs. There are

RSC Advances Accepted Manuscript

only a few visible r-MWCNTs, highlighted by yellow circles that have been pulled out from the epoxy matrix during the fracture process.

By comparison, the MWCNT@SiO_2/epoxy composite shows improved dispersion and homogeneity on the fractured surface (Fig. 4f). Most of the MWCNT@SiO_2 are embedded in the epoxy matrix, and fewer of them are pulled out from the matrix as compared to the r-MWCNT/epoxy composite, suggesting that stronger interfacial bonding exists between epoxide/hydroxyl groups in the epoxy matrix and carbonyl/carboxylic groups on MWCNT@SiO_2. Consequently, the compatibility and interfacial adhesion between MWCNT@SiO_2 and epoxy are improved through the silica coating of r-MWCNTs. As interpreted by Cui *et al*. [9], another cause for this behavior may be the uniform silica shell serving as a physical intermediate layer between the MWCNT and the epoxy matrix, minimizing tube-tube aggregation.

3.3 Curing behavior of composites

3.3.1 Isothermal FT-IR analysis

The effect of the silica layer on the MWCNT surface on the curing behavior of epoxy composites is quite important for the final properties of the composite. Here, FT-IR is used to investigate the curing reaction rate of neat epoxy and MWCNT/epoxy composites. Fig. 5a and b show the FT-IR spectra of the neat epoxy and epoxy composites cured at 150 ºC at different times.

In both systems, the characteristic stretching features of epoxy groups at 915 cm^{-1} and 923 cm^{-1} decrease in intensity gradually; the signatures of the anhydride group at 1776 cm^{-1} and 1838 cm^{-1} decrease quickly with reaction time from the beginning of the reaction until 60 min. Peaks at 1606, 1581, 1508 and 1456 cm^{-1} originate from bond stretching of the benzene ring from anhydride MeTHPA. From equation (1), the

RSC Advances Accepted Manuscript

extent of reaction (α) can be calculated by the consumption of the characteristic peak of the epoxy group at 915 cm^{-1}, with the stretching vibration peak of benzene at 1606 cm^{-1} chosen as the reference peak [33-34]:

$$\alpha = 1 - \frac{A'_{915}/A'_{1606}}{A_{915}/A_{1606}} \quad (1)$$

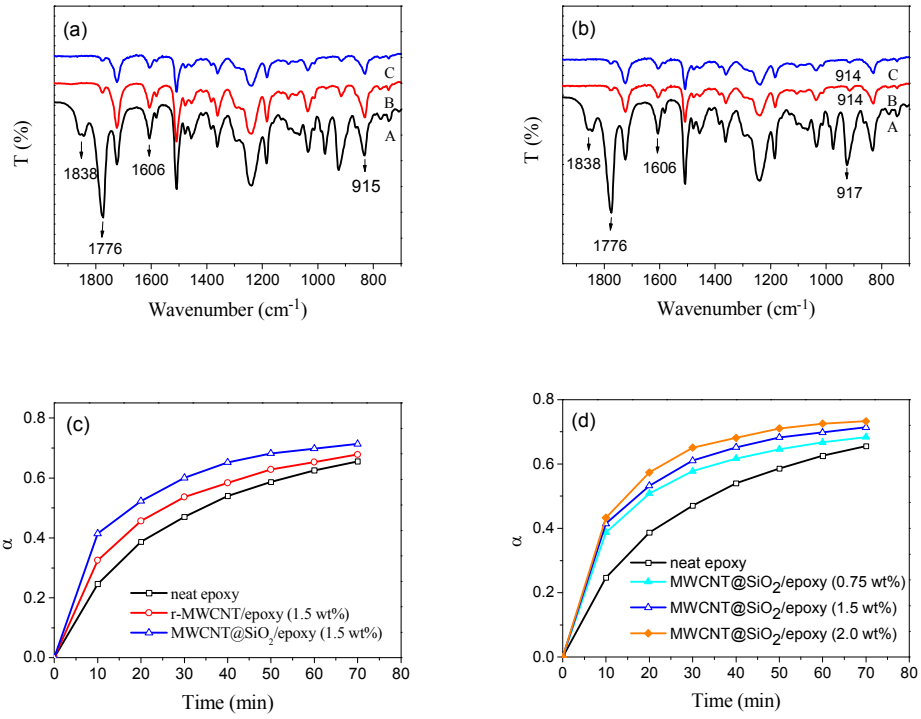

Fig. 5 FT-IR spectra of (a) neat epoxy and (b) MWCNT@SiO_2/epoxy composites, cured at 150 ºC for (A) 0 min, (B) 30 min and (C) 60 min; (c) reaction conversion versus time for neat epoxy and epoxy composites cured at 150 ºC and (d) for MWCNT@SiO_2/epoxy composites with different contents of MWCNT@SiO_2, cured at 150 ºC.

From Fig. 5c and d, it can be seen that the reaction rate curves are typically autocatalytic, with maximum rates of reaction occurring immediately after the start of the reaction [28]. From Fig. 5c, it is found that the curing reaction rate of each

RSC Advances Accepted Manuscript

MWCNT/epoxy composite is faster than the neat epoxy resin. Moreover, when the r-MWCNTs were coated with silica, the curing reaction conversion and rate are increased significantly. It is believed that the -OH groups on the surface of silica-coated MWCNTs exert a catalytic effect for epoxide ring opening [28].

Furthermore, the initial reaction rates are affected by the presence and content of r-MWCNTs and MWCNT@SiO_2, increasing as the MWCNT@SiO_2 content increases, as shown in Fig. 5d. The influence of MWCNT@SiO_2 content on the curing reaction conversion and rate is significant, relative to the curing reaction of neat epoxy resin and the r-MWCNT-filled epoxy resin. This can be explained by the consideration of the hydroxyl groups at the silica surface, induced by the sol-gel process, that hydrogen bond with the epoxide ring of the matrix and act as an accelerant to increase the curing reaction rate. As the MWCNT@SiO_2 content is increased, the larger content of surface hydroxyl groups available for hydrogen bonding will lead to an increased conversion rate.

3.3.2 Nonisothermal DSC analysis

Nonisothermal DSC measurements were also carried out to further study the effect of the silica coating on the composites' curing behavior. Fig. 6a presents DSC curves of neat epoxy and epoxy composites at a heating rate of 10 ºC/min. The peak maximum temperatures (T_p) of the epoxy curing reactions are summarized in Table 1.

At a given heating rate, the peak temperature of the exothermic curve decreased slightly when r-MWCNTs or MWCNT@SiO_2 are added (similar to the results reported by literature examples [29,31,32]), and this phenomenon indicated that -OH groups on the surface of MWCNTs may accelerate the curing reaction, which is consistent with the results of FT-IR.

RSC Advances Accepted Manuscript

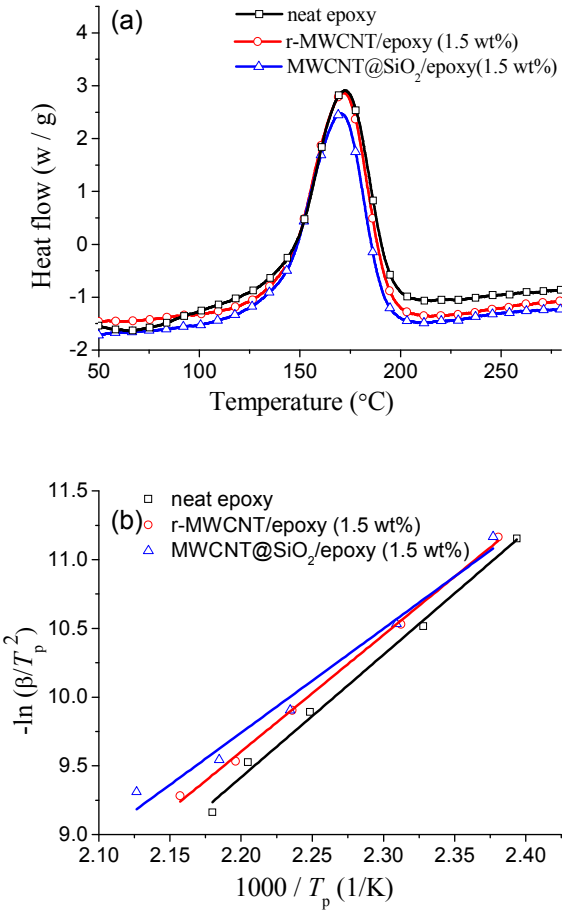

Fig. 6 (a) DSC curves of neat epoxy and epoxy composites at a heating rate of 10 ºC/min; (b) a plot of -ln (β/T_p^2) versus 1000/T_p for Arrhenius behavior of epoxy curing based on the DSC results.

Table 1 T_p values (K) for epoxy and composites from the DSC measurements at different heating rates.

Material	T_p, 2.5 K/min	T_p, 5 K/min	T_p, 10 K/min	T_p, 15 K/min	T_p, 20 K/min
neat epoxy	419.2	432.5	445.4	453.7	458.5
r-MWCNT/epoxy (1.5/100)	418.4	430.4	444.2	451.6	457.3
MWCNT@SiO_2/epoxy(1.5/100)	416.5	429.4	442.1	448.5	455.4

RSC Advances Accepted Manuscript

A plot of –ln (β/T_p^2) versus $1000/T_p$, which according to the Kissinger equation [43](2) allows the determination of the apparent activation energy for curing, is shown in Fig. 6b.

$$-\mathrm{d}ln(\beta/T_p^2)/\mathrm{d}(1/T_p) = E_a/R \quad (2)$$

where β is a constant heating rate, E_a is the activation energy, and R is the gas constant (8.314 J mol^{-1} K^{-1}).

The activation energy calculated for neat epoxy, r-MWCNT/epoxy (1.5 wt%) and MWCNT@SiO_2/epoxy (1.5 wt%) composites are 77.3 kJ/mol, 71.2 kJ/mol and 62.7 kJ/mol, respectively. This indicates that the introduction of MWCNTs decreases the activation energy of the curing reaction and agrees with the results reported by Xie *et al.* [28]. This decrease of the activation energy may be explained by the consideration that the carboxyl groups on the r-MWCNT surface and the hydroxyl groups enriched on the MWCNT@SiO_2 surface form a hydrogen bond with the oxirane ring, which decreases the energy barrier of curing and accelerates the cross-linking reaction. This result is consistent with the results from FT-IR measurements. As expected, the effect of the presence of hydroxyl groups on decreasing the activation energy is more significant than that of the carbonyl group. As suggested by Lavorgna *et al.*, some reactive groups present in the silica-coated nanotubes such as SiOH may catalyze the epoxy crosslinking reactions [26].

3.4 Physical and thermomechanical properties of epoxy composites

3.4.1 Electrical resistivity

MWCNTs are widely used to improve the electrical conductivity of industrial composites. However, electrical insulation is required for the electronic packaging applications discussed in this report. Herein, silica was coated on the surface of r-

RSC Advances Accepted Manuscript

MWCNTs, and the effect of MWCNT content on the electrical resistivity of the epoxy composites was studied, with the results shown in Fig. 7. The electrical resistivity of the epoxy composites with 1.5 wt% r-MWCNTs decreases sharply by three orders of magnitude, with respect to the neat epoxy, from 2.3×10^{15} to 1.9×10^{12} Ω cm, while the electrical resistivity of the epoxy composites with the same content of MWCNT@SiO_2 exhibits a smaller decrease relative to neat epoxy, from 2.3×10^{15} to 3.1×10^{13} Ω cm. Specifically for the MWCNT@SiO_2 content range from 0.75 to 1.5 wt%, the value of electrical resistivity is nearly constant.

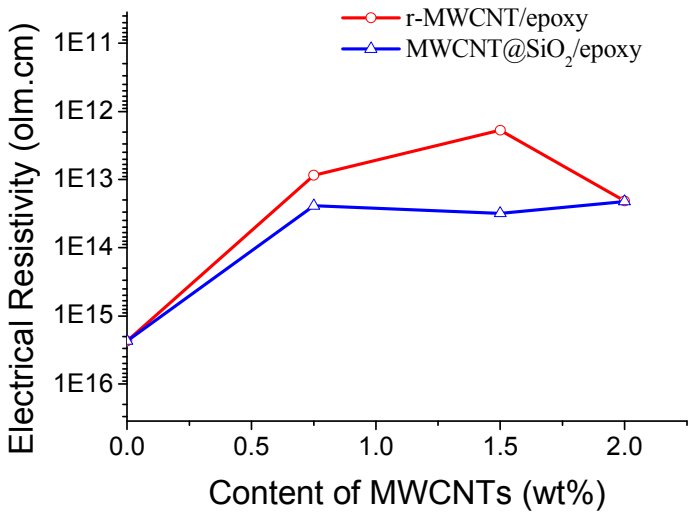

Fig. 7 Electrical resistivity for both epoxy composites as a function of MWCNTs content.

When the concentration of r-MWCNTs is increased to 2.0 wt%, the dispersion morphology becomes coarsened due to nanotube aggregation, the electrically conductive network is broken, and the electrical resistivity increases again partially. For the MWCNT@SiO_2/epoxy composites, the electrical resistivity remains nearly

RSC Advances Accepted Manuscript

constant once the nanotube concentration exceeds 0.75 wt%. The difference between the two composites' electrical resistivity behavior is explained by the consideration that the silica shell for MWCNT@SiO_2/epoxy composites can prevent MWCNTs from coming into physical contact and aggregating, therefore resulting in a less interconnecting network that effectively blocks the electron movement between MWCNTs [9].

3.4.2 Thermal conductivity

The highest reported nanotube thermal conductivities are on the order of 10^3 W/(m K), while typical polymers have κ~ 0.1 W/(m K). For an application of epoxy in electronic packaging, the excellent thermal conductivity of nanotubes leads to early expectations that it will enhance the thermal conductivity of epoxy nanocomposites [4]. Fig. 8 reveals that the dispersion of 0.75, 1.5 and 2.0 wt% MWCNTs into epoxy resin does indeed increase the thermal conductivity. In addition, the thermal conductivity of epoxy composites increases as the content of MWCNTs increases. Interestingly, the r-MWCNTs composites exhibit a smaller enhancement than MWCNTs@SiO_2 in spite of the low thermal conductivity of the amorphous silica coating. For the r-MWCNT/epoxy composites, the thermal conductivity increases by 63.6% from 0.11 for neat epoxy resin to 0.18 W/mk at 2.0 wt% of r-MWCNTs. For the MWCNT@SiO_2/epoxy composites, a significant improvement in the thermal conductivity of 127% from 0.11 to 0.25 W/mk was observed.

Phonons entering the MWCNT/epoxy composite are much more likely to travel through the matrix than electrons because the contrast in thermal conductivity ($\kappa_{nanotube}/\kappa_{polymer}$) is ~$10^4$ in comparison to the electrical conductivity contrast ($\sigma_{nanotube}/\sigma_{polymer}$) of ~$10^{15}$-$10^{19}$ [4]. Therefore, the difference in thermal conductivity between r-MWCNT/epoxy and MWCNT@SiO_2/epoxy composites indicates that the

RSC Advances Accepted Manuscript

silica shell both improves the interfacial heat transport between the epoxy matrix and the MWCNT@SiO_2 and leads to better dispersion of MWCNT@SiO_2 in the epoxy matrix, implying that the improved interfacial adhesion and heat transport are both factors leading to the enhanced thermal conductivity for epoxy composites containing silica-coated MWCNTs.

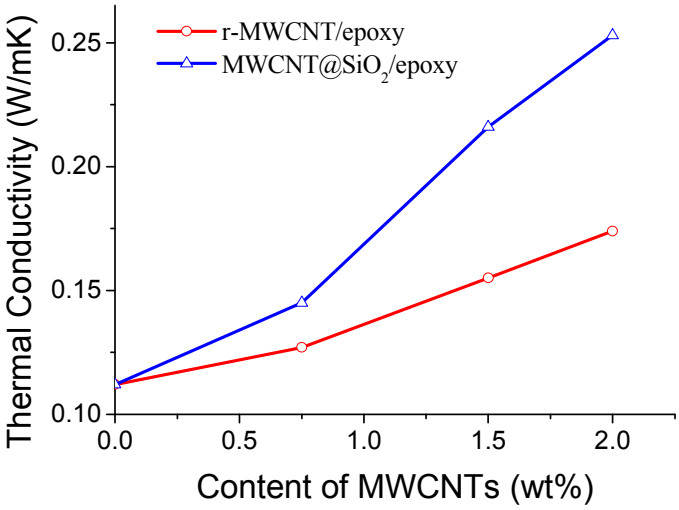

Fig. 8 Thermal conductivities for epoxy composites as a function of content of r-MWCNTs and MWCNT@SiO_2.

3.4.3 Thermomechanical properties

The improved interfacial interactions between the functionalized MWCNTs and epoxy matrix also result in enhancements of glassy and rubbery moduli for such composites [26]. The storage modulus (E') and the loss factor (tan δ) of neat epoxy and epoxy composites with different MWCNTs at a concentration of 0.75 wt% are shown in Fig. 9a. It is found that the incorporation of MWCNTs into the epoxy system results in an increase in storage modulus E', and the E' of samples increases

RSC Advances Accepted Manuscript

gradually in the order of neat epoxy, r-MWCNT/epoxy, and MWCNT@SiO_2/epoxy composites in the glassy plateau region. This trend may be explained by the contribution of the hydroxyl groups, at the silica surface, to the improvement of both the compatibility of the filler with the epoxy matrix and the more effective dispersion of MWCNT@SiO_2 in the epoxy matrix [9,23].

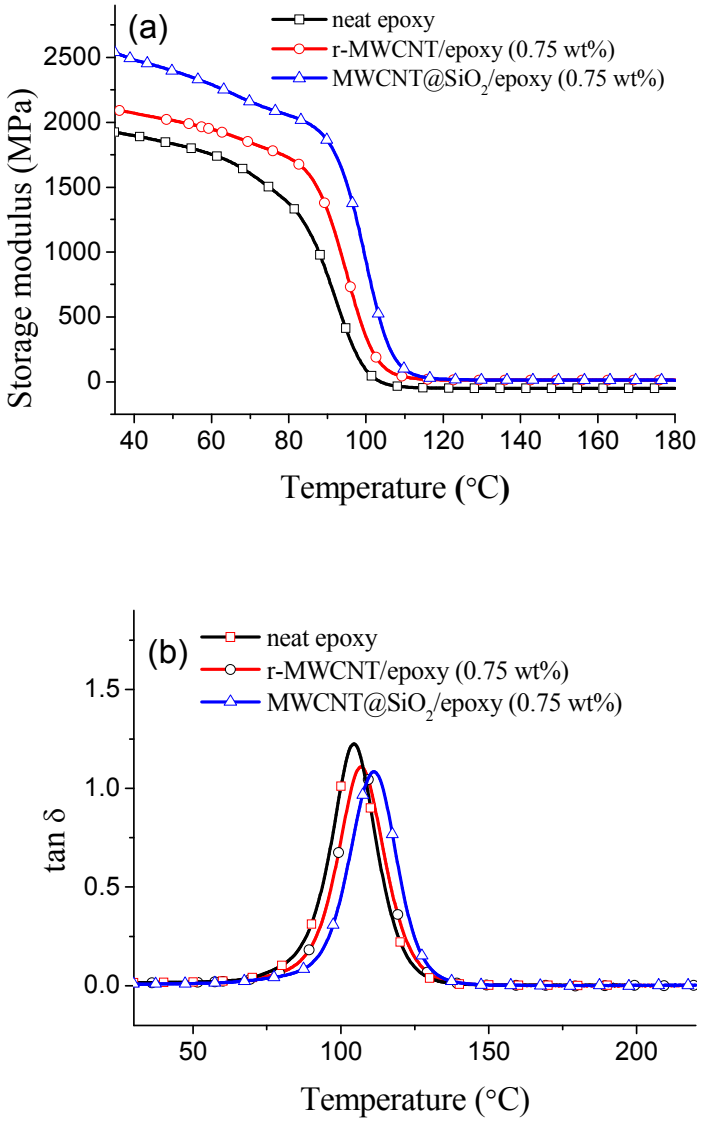

Fig. 9 (a) Storage modulus (E') and (b) loss factor (tan δ) of neat epoxy and epoxy composites with 0.75 wt% of either r-MWCNTs or MWCNT@SiO_2.

RSC Advances Accepted Manuscript

The glass transition temperature (T_g) is closely linked to the thermomechanical stability and is thus a critical property that dictates the potential application of a given epoxy resin [30]. The tan δ, equal to the ratio of the loss modulus to the storage modulus, as a function of the temperature, for neat epoxy and composites with 0.75 wt% of MWCNTs is presented in Fig. 9b. The T_g is obtained from the peak maximum position of the temperature-dependent tan δ curve. The T_g of r-MWCNT/epoxy and MWCNT@SiO_2/epoxy composites shifts to a slightly higher temperature, with the MWCNT@SiO_2/epoxy composites exhibiting the highest glass transition temperature. This result agrees with literature reports [9,20,23]. The addition of MWCNT@SiO_2 in the epoxy resin increases T_g to 111 ºC from 104 ºC for neat epoxy, compared with the increase in T_g to 107 ºC for r-MWCNT/epoxy composites. This difference in the glass transition is the result of the strong interaction between the hydroxyl groups enriched on the silica shell of MWCNT@SiO_2 and the epoxy matrix, that may further harden the composite by catalyzing the epoxy crosslinking reaction [24,26], therefore enhancing the interfacial adhesion and restricting the segmental motion of the epoxy chains under shear. This finding is also in agreement with the accelerated curing observed for composites containing silica-functionalized MWCNTs from FT-IR and DSC results.

4. Conclusions

A uniform silica shell was successfully coated on the surface of MWCNTs by a sol-gel process, and the MWCNT@SiO_2 was incorporated into an epoxy matrix as the filler. The effects of silica-functionalized MWCNT addition on the curing behavior, electrical and thermal conductivity, and thermomechanical properties of epoxy-based

RSC Advances Accepted Manuscript

composites were studied. The results highlight that the curing reaction conversion and rate increased with the introduction of r-MWCNTs and MWCNT@SiO_2, while the activation energy decreased. The silica shell of the functionalized MWCNTs improved the interfacial bonding and resulted in a better dispersion of MWCNTs in the matrix. Meanwhile, the thermomechanical properties and thermal conductivity were improved significantly by introduction of MWCNT@SiO_2 into the epoxy resin matrix. Moreover, the MWCNT@SiO_2/epoxy composites retained a high electrical resistivity simultaneously. Therefore, the systematic study of the incorporation of functionalized MWCNTs, as a function of composite concentration, on the curing behavior, electrical and thermal conductivity, and thermomechanical properties presented here provides a processing window for obtaining each optimized property that is needed in electronic packaging applications.

Acknowledgments

The authors wish to thank the Shanghai Municipal Education Commission (Overseas Visiting Scholar Project 20120407); Shanghai Young Teachers' Training-funded Projects (ZZGJD13018); Shanghai University of Engineering Science Developing funding (grant 2011XZ04), start-up project funding (grant 0501-13-018) and Interdisciplinary Subject Construction funding (grant 2012SCX005).

References

1 S. Iijima, *Nature* 1991, 354, 56.

2 E. Dervishi, Z. R. Li, Y. Xu, V. Saini, A. R. Biris, D. Lupu and A. S. Biris, *Particulate Science and Technology*, 2009, 27, 107.

3 P. C. Ma, N. A. Siddiqui, G. Marom and J. K. Kim, *Composites Part A*, 2010, 41,

RSC Advances Accepted Manuscript

1345.

4 M. Moniruzzaman and K. I. Winey, *Macromolecules*, 2006, 39, 5194.

5 J. N. Coleman, U. Khan, W. J. Blau and Y. K. Gun'ko, *Carbon*, 2006, 44, 1624.

6 S. Berber, Y. K. Kwon and D. Tomanek, *Physical Review Letters*, 2000, 84, 4613.

7 P. Kim, L. Shi, A. Majumdar and P. L. McEuen, *Physical Review Letters*, 2001, 87, 4.

8 S. R. Wang, R. Liang, B. Wang and C. Zhang, *Carbon*, 2009, 47, 53.

9 W. Cui, F. P. Du, J. C. Zhao, W. Zhang, Y. K. Yang, X. L. Xie and Y. W. Mai, *Carbon*, 2011, 49, 495.

10 A. Allaoui, S. Bai, H. M. Cheng and J. B. Bai, *Composites Science and Technology*, 2002, 62, 1993.

11 J. A. Kim, D. G. Seong, T. J. Kang and J. R. Youn, *Carbon*, 2006, 44, 1898.

12 F. H. Gojny and K. Schulte, *Composites Science and Technology*, 2004, 64, 2303.

13 P. C. Ma, S. Y. Mo, B. Z. Tang and J. K. Kim, *Carbon*, 2010, 48, 1824.

14 K. Yang, M. Y. Gu, Y. P. Guo, X. F. Pan and G. H. Mu, *Carbon*, 2009, 47, 1723.

15 S. Y. Yang, C. C. M. Ma, C. C. Teng, Y. W. Huang, S. H. Liao, Y. L. Huang, H. W. Tien, T. M. Lee and K. C. Chiou, *Carbon*, 2010, 48, 592.

16 Y. S. Song and J. R. Youn, *Carbon*, 2005, 43, 1378.

17 F. H. Gojny, M. H. G. Wichman, B. Fiedler, I. A. Kinloch, W. Bauhofer, A. H. Windle and K. Schulte, *Polymer*, 2006, 47, 2036.

18 A. Moisala, Q. Li, I. A. Kinloch and A. H. Windle, *Composites Science and Technology*, 2006, 66, 1285.

19 F. H. Gojny, M. H. G. Wichmann, U. Kopke, B. Fiedler and K. Schulte, *Composites Science and Technology*, 2004, 64, 2363.

RSC Advances Accepted Manuscript

20 Y. Geng, M. Y. Liu, J. Li, X. M. Shi and J. K. Kim, *Composites Part A*, 2008, 39, 1876.

21 M. T. Kim, K. Y. Rhee, S. J. Park and D. Hui, *Composites Part B*, 2012, 43, 2298.

22 L. C. Tang, Y. J. Wan, K. Peng, Y. B. Pei, L. B. Wu, L. M. Chen, L. J. Shu, J. X. Jiang and G. Q. Lai, *Composites Part A*, 2013, 45, 95.

23 M. H. Chung, L. M. Chen, W. H. Wang, Y. S. Lai, P. F. Yang and H. P. Lin, *Journal of the Taiwan Institute of Chemical Engineers*, 2014, 45, 2813.

24 P. C. Ma, J. K. Kim and B. Z. Tang, *Composites Science and Technology*, 2007, 67, 2965.

25 J. Kathi, K. Y. Rhee and J. H. Lee, *Composites Part A*, 2009, 40, 800.

26 M. Lavorgna, V. Romeo, A. Martone, M. Zarrelli, M. Giordano, G. G. Buonocore, M. Z. Qu, G. X. Fei and H. S. Xia, *European Polymer Journal*, 2013, 49, 428.

27 D. Puglia, L. Valentini and J. M. Kenny, *Journal of Applied Polymer Science*, 2003, 88, 452.

28 H. F. Xie, B. H. Liu, Z. R. Yuan, J. Y. Shen and R. S. Cheng, *Journal of Polymer Science Part B*, 2004, 42, 3701.

29 K. Tao, S. Y. Yang, J. C. Grunlan, Y. S. Kim, B. Dang, Y. J. Deng, R. L. Thomas, B. L. Wilson and X. Wei, *Journal of Applied Polymer Science*, 2006, 102, 5248.

30 A. Allaoui and N. El Bounia, *Express Polymer Letters*, 2009, 3, 588.

31 T. L. Zhou, X. Wang, X. H. Liu and D. S. Xiong, *Carbon*, 2009, 47, 1112.

32 L. J. Cui, Y. B. Wang, W. J. Xiu, W. Y. Wang, L. H. Xu, X. B. Xu, Y. Meng, L. Y. Li, J. Gao, L. T. Chen and H. Z. Geng, *Materials & Design*, 2013, 49, 279.

33 L. Guadagno, B. D. Vivo, A. D. Bartolomeo, P. Lamberti, A. Sorrentino, V. Tucci, L. Vertuccio and V. Vittoria*, Carbon*, 2011, 49, 1919.

34 K. Yang, M. Y. Gu and Y. P. Jin, *Journal of Applied Polymer Science*, 2008, 110,

RSC Advances Accepted Manuscript

2980.

35 K. Yang, M. Y. Gu, Y. P. Jin, G. H. Mu and X. F. Pan, *Composites Part A,* 2008, 39, 1670.

36 W. J. Choi, R. L. Powell and D. S. Kim, *Polymer Composites*, 2009, 30, 415.

37 F. Wang, S. Q. Li, J. W. Wang and J. Xiao, *High Performance Polymers*, 2012, 24, 97.

38 J. Rocks, L. Rintoul, F. Vohwinkel and G. George, *Polymer*, 2004, 45, 6799.

39 H. Miyagawa and L. T. Drzal, *Polymer*, 2004, 45, 5163.

40 X. L. Jia, G. Li, B. Y. Liu, Y. M. Luo, G. Yang and X. P. Yang, *Composites Part A*, 2013, 48, 101.

41 S. J. Guo, S. J. Dong and E. K. Wang, *J. Phys. Chem. C*, 2008, 112, 2389.

42 C. Graf, D. L. J. Vossen, A. Imhof and A. Blaaderen, *Langmuir*, 2003, 19, 6693.

43 R. L. Blaine and H. E. Kissinger, *Thermochimica Acta*, 2012, 540, 1.

RSC Advances Accepted Manuscript

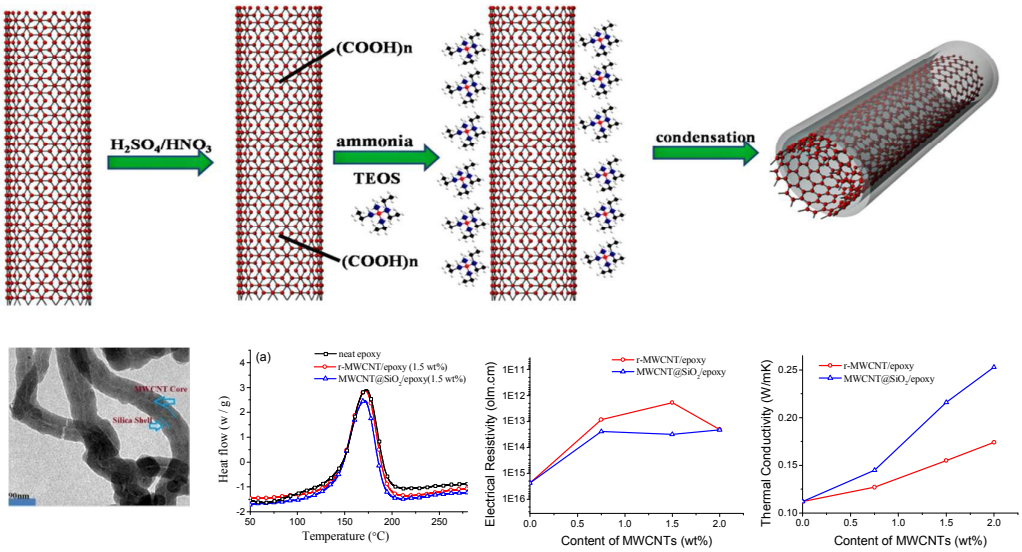

Carbon nanotubes coated with silica and resultant effects on epoxy composites

RSC Advances Accepted Manuscript